Journal of Electronic Materials (2024) 53:5916–5925
https://doi.org/10.1007/s11664-024-11117-6

28TH INTERNATIONAL CONFERENCE ON NUCLEAR TRACKS AND RADIATION MEASUREMENTS

An Improved CVD Design for Graphene Growth and Transfer Improvements

Gargi Dhiman[1] · Shalendra Kumar[1] · Rajesh Kumar[2] · Ranjeet Brajpuriya[1]

Received: 24 January 2024 / Accepted: 10 April 2024 / Published online: 8 May 2024

Abstract
Contamination-free graphene presents vast potential in diverse energy applications, encompassing storage, conversion, harvesting, and catalysis. Ongoing endeavors to ensure graphene's purity are poised to unlock fresh prospects for advancing sustainable and efficient energy technologies. Despite the chemical vapor deposition (CVD) method's promise in delivering large-area, high-crystallinity graphene with unique properties, industrial-scale production remains a challenge. Issues surrounding the uniformity and reproducibility of graphene films persist, particularly when synthesized in quartz furnaces, leading to unintended particle contamination that alters growth processes and graphene properties. This study delves into the formation and origins of these contaminants during growth. The authors propose modifying quartz furnace layouts to mitigate sample contamination and achieve clean, uniform graphene films across large areas. Evaluation using scanning electron microscopy (SEM), x-ray photoelectron spectroscopy (XPS), and Raman spectrometry elucidated the characteristics of both as-grown and transferred graphene films.

Keywords Graphene · CVD · quartz furnaces · transfer · Raman · XPS · SEM

Introduction

Contamination-free graphene, a one-atom-thin carbon nanosheet renowned for its exceptional properties, holds enormous potential across diverse energy applications and industries. Recognized as a "miracle material," graphene exhibits remarkable attributes, including optical transparency, flexibility, large surface area, outstanding electrical conductivity, ultra-lightweight nature, and chemical inertness. Its eco-friendly and renewable characteristics position graphene as a transformative element for future industries.[1] In electronics, it enables the fabrication of faster and more efficient devices such as field-effect transistors (FETs), solar generators, high-performance wind turbines, ultrafast computers, and flexible electronic displays. Graphene's large surface area and light-transmitting capabilities make it promising for solar cells. In energy storage, graphene-based batteries and supercapacitors could revolutionize the sector by providing durable and effective solutions.[2] The medical field benefits from graphene's biocompatibility and high surface area, making it an excellent candidate for drug delivery systems and biosensors. Its mechanical strength, flexibility, and impermeability contribute to applications in aircraft manufacturing, space vehicles, water filtration, and sports equipment.[3]

However, realizing graphene's potential on a large scale demands cost-effective, contamination-free production on substrates compatible with electronic devices.[4] Challenges such as scalability, integration, bandgap engineering, and environmental impact need to be addressed.[5] Prioritizing optimization in synthesis and transfer methodologies is essential for enhancing efficiency and control, ensuring graphene's widespread utilization in various substrates and industries.[6,7]

✉ Gargi Dhiman
gargidhimaan@gmail.com

✉ Ranjeet Brajpuriya
ranjeetbjp1@gmail.com

[1] Department of Physics, UPES, Dehradun, Uttarakhand 248007, India

[2] University School of Basic and Applied Sciences, Guru Gobind Singh Indraprastha University, New Delhi 110078, India

Some recent work has been done on improving the quality of graphene. Zhaoninh et al. achieved scalable production of large-area graphene films on metal foils and introduced a crack-free and clean transfer of graphene wafers onto silicon wafers.[8] Haina et al. demonstrated direct growth of graphene on Si-wafer by optimizing H_2 dosage and methanol to reduce the graphene-substrate interaction and fabricated high-performance graphene-based FETs.[9] Bingzhi et al. reported large-area and direct graphene synthesis over fused quartz as a functional substrate via chemical vapor deposition.[10] Bei et al. reported the successful growth of wrinkle-free, ultra-flat graphene on a glass substrate.[11] Additionally, Li et al. presented a wafer-scale synthesis of graphene on a sapphire substrate for application in nanoelectronic devices.[12]

Graphene Growth (CVD Technique and the Variables Affecting Growth)

In 2004, Professors Andre Geim and Konstantin Novoselov's groundbreaking discovery of high-quality monolayer graphene using the Scotch tape method marked the beginning of extensive research on this remarkable material.[13] Awarded the 2010 Nobel Prize in Physics, their work ushered in a new era of technological exploration.[14] Various graphene synthesis methods, including mechanical and electrochemical exfoliation, epitaxial growth, and arc discharge, each have distinct advantages and drawbacks. While mechanical exfoliation offers high quality at a low cost, it lacks scalability.[15] Chemical and electrochemical methods are scalable but introduce structural defects.[16] Epitaxial growth produces high quality but restricts substrate choice and increases costs.[17] To overcome these limitations, researchers are actively exploring chemical vapor deposition (CVD) due to its versatility, scalability, and economic viability. Despite some drawbacks, CVD stands out as the most promising large-scale graphene processing method, continually evolving to achieve high-quality graphene.[18] In the CVD process, gaseous species react at high temperatures in the presence of metallic catalysts, influencing graphene growth on metals through factors like substrate, carbon solubility, crystal structure, gas composition, and thermodynamics.[19,20] Contamination sources and extent can vary, necessitating a thorough understanding and implementation of mitigation strategies for high-quality graphene films.[21]

To study the surface morphology and growth mechanisms of graphene, numerous metal catalytic substrates have been explored to date, including Ni, Cu, Pt, Pd, Au, and Ru.[22] Among metal catalytic substrates, Cu is preferred for its catalytic properties, lattice structure resembling graphene, availability, and cost efficiency. It promotes graphene nucleation, allowing clean transfer for device integration.[23,24]

The choice of a carbon precursor is crucial, and ethanol emerges as an effective option, surpassing methane in efficiency, safety, affordability, and ease of treatment. Ethanol's weak oxidizing nature contributes to rapid growth and allows continuous graphene layer formation, unlike methane. Ethanol's oxygen content enhances graphene quality.[25–27]

Hydrogen's role in CVD involves cleaning the metallic substrate and tuning graphene film thickness, crystallinity, and quality by optimizing flow rate and pressure. Higher hydrogen flow rates promote highly crystalline monolayer graphene.[28]

Temperature significantly influences graphene synthesis, impacting film quality, structure, and growth kinetics. Higher temperatures accelerate growth rates and reduce substrate surface roughness, enhancing mobility and lowering defect density in the graphene film.[29]

In conclusion, the synthesis of high-quality graphene involves a complex interplay of various parameters and methodologies, with CVD emerging as a leading contender for large-scale production. Ongoing research aims to refine and optimize these processes to unlock the full potential of graphene in diverse applications.

Potential Sources of Contaminants during the CVD Growth Process

While chemical vapor deposition (CVD) is a widely employed technique for growing high-quality, defect-free graphene, achieving continuous and monolayer films across large areas poses challenges. Even slight fluctuations in temperature, pressure, and gas flow can lead to uneven growth and defects in graphene layers.[30] Additionally, precursor gases undergo chemical reactions producing toxic byproducts that can impact the environment. Contaminants are identified when synthesizing graphene on copper foil, especially at extremely high temperatures below copper's melting point using hot-wall or cold-wall metal reactors.[31] During high-temperature growth, the quartz tube material may experience significant strain, potentially contaminating graphene, especially in the presence of oxidants.[32] The transition from α-quartz to β-quartz during the growth process facilitates the migration of Cu atoms within the quartz material, impacting density and allowing carbon and copper to permeate throughout the tube. The practical implications of this phenomenon in graphene production highlight the potential complications in terms of cost and reproducibility, particularly related to quartz tube and vessel aging.[33–35] The current paper addresses contamination issues in graphene production, proposing a solution using a quartz reactor and a vessel with an advanced design. The authors present a quick, annealing-free, and chemical etching-free method for transferring high-quality CVD graphene onto flexible surfaces. The graphene films, both as-grown and transferred, undergo analysis using spectroscopic methods such as

x-ray photoelectron spectroscopy (XPS), scanning electron microscopy (SEM), and Raman spectroscopy.

Methodology

Low-pressure CVD was used to synthesize graphene on a polycrystalline Cu foil with a thickness of 25 µm and a purity of 99.95%. The formation of homogeneous graphene film over Cu requires a clean substrate, and therefore, anti-corrosive treatment is applied to the Cu foil surface to avoid oxidation. Even the foil that is resistant to corrosion has a thin layer of Cu oxide on its surface. To ensure that the growth of graphene is of high grade, these Cu oxide layers have been removed from the surface by cleaning Cu foils ultrasonically at room temperature (RT) in acetone and ethanol for around 15 min before graphene formation (see Fig 1a). After substrate cleaning, a quartz sample holder containing Cu foils is inserted within the chemical vapor deposition chamber, thereafter annealing for 20 min at 1000°C with Ar (20 sccm) and H_2 (20 sccm). It can be seen that annealing at higher temperatures increases the crystallite size and removes native oxide from the copper surface (see Fig. 1b). After that, ethanol (C_2H_5OH), a gaseous carbon which had been diluted in Ar (0.1% in 20 sccm of Ar) and then added to the tube with hydrogen gas (100 sccm) for 30 min to grow graphene. Eventually, the film was taken out of the heated area and allowed to cool under an Ar flow before further inspection. Figure 2a schematically shows the temperature–time profile during the CVD growth process and Fig. 2b summarizes the graphene growth mechanism on Cu foil by the CVD method.

SEM, Raman spectroscopy, and XPS are used to characterize graphene quality, microstructure, number of layers, and defects. Mg-Kα radiations were used for XPS measurements in a vacuum greater than 1.33×10^{-10} kPa. For a survey, the instrument pass energy was 50 eV, and for a thorough scan, it was 20 eV. To maximize surface sensitivity, all XPS spectra are taken at 30° with 15 Å depth analysis. A Zeiss (formerly LEO) 1530 field emission scanning electron microscope was used to look for contaminants and determine the surface morphology of both as-grown and transferred samples. Using a refractive index (RI) confocal Raman microscope, an excitation line of 532 nm (2.33 eV), a 20× objective lens, and an incident power of 1 mW, spectra of graphene transferred to Si/SiO_2 substrates were obtained.

Results and Discussion

The inset of Fig. 3 depicts a high-resolution SEM image of a graphene film developed at a temperature of 1000°C for 30 min using a conventional old quartz tube. During graphene growth, the authors noticed widespread microscopic white sphere-shaped spots contaminating the entire Cu surface. Similar characteristics are frequently observed in many published research articles to varying degrees,[36,37] but they fail to explain the nature of the same. This kind of contamination appears in typical CVD-grown graphene sheets produced in traditional quartz tube furnaces, and it is frequently associated with oxidizing precursors. The inset of Fig. 3 also displays an image depicting the regularly used old quartz tube. The center of the tube is extensively contaminated with copper (Cu) atoms. The varying colors observed at different sections of the tube can be attributed to the distinct temperatures experienced in those specific regions during the growth process. However, when the film was developed using a newly assembled, sterile quartz tube, there was no evidence of surface contamination (see Fig. 5 inset). The nature of these traits when using methane has

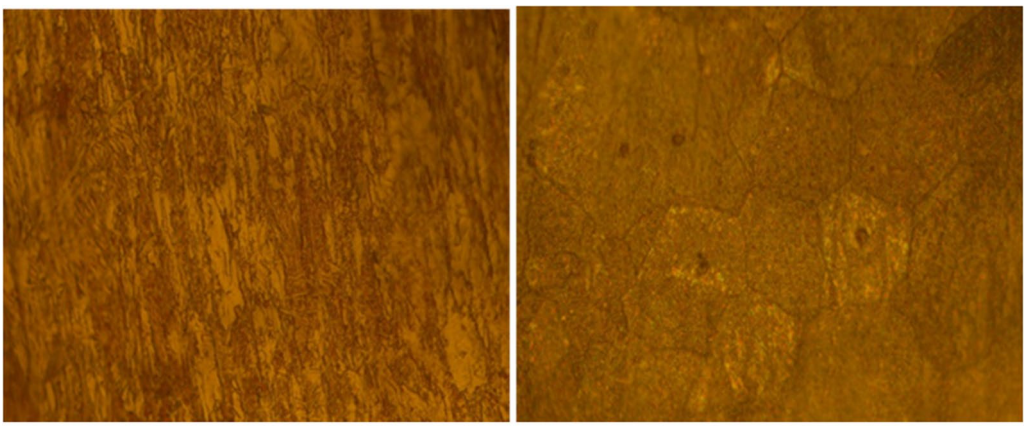

Fig. 1 (a) Optical micrographs of pretreated (left) and (b) annealed copper foil at 1000°C (right).

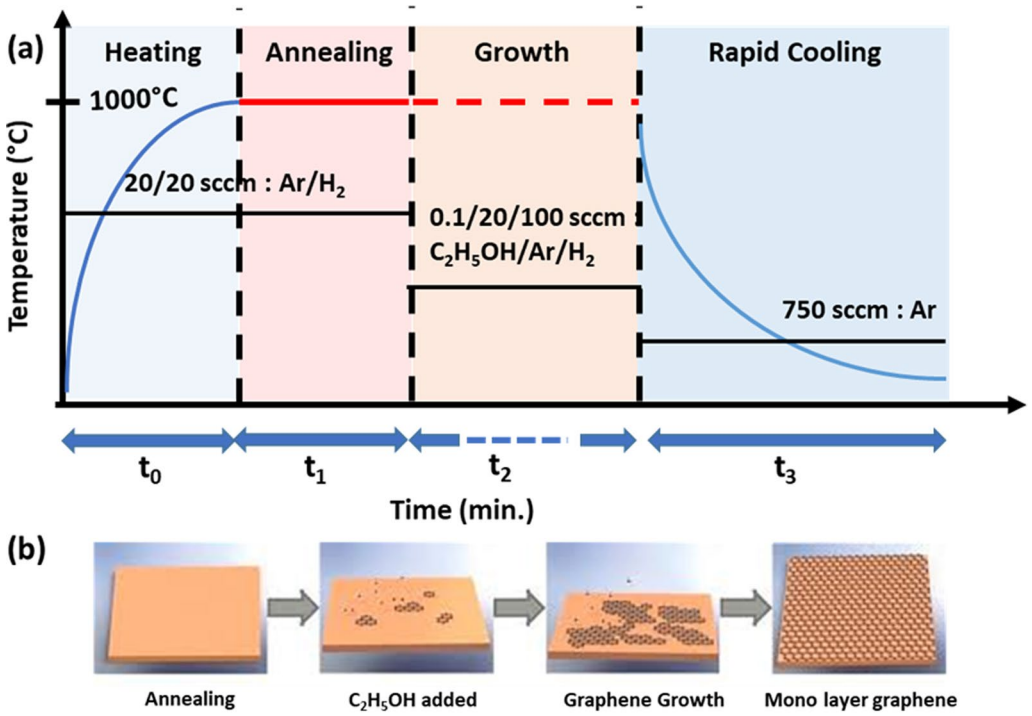

Fig. 2 (a) Temperature–time profile during CVD growth process (sample insertion and heating [t_0), insertion in the hot zone and annealing (t_1), growth (t_2), extraction from the hot zone and rapid cooling (t_3)], and (b) graphene growth mechanism on Cu foil by the CVD method.

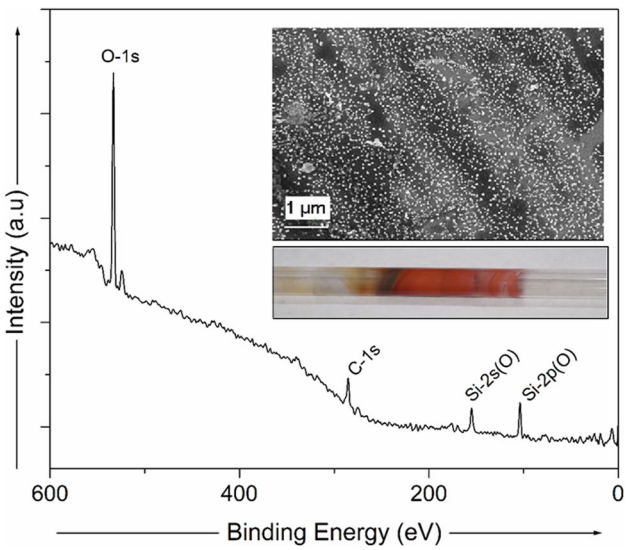

Fig. 3 XPS survey scan of graphene film/Cu deposited using a regularly used old quartz tube (inset shows the SEM image of the corresponding contaminated film).

been described and discussed by Ruiz et al. The impurities are identified by the authors as SiO_x clusters, which originate from the quartz walls when Cu atoms diffuse inside the tube walls and in the boat supporting the Cu foil at the phase transition temperature between α and β quartz.[32] Since this is a slow process, the effect is thus connected to the degradation of the quartz tube vessel; nevertheless, our experimental results show that the effect is greatly reduced when a new tube is utilized.

X-ray photoelectron spectroscopy (XPS) studies were carried out to identify the white, sphere-like impurities. The full scan of the corresponding surfaces is shown in Fig. 3, which reveals a lack of the anticipated prominent peaks associated with carbon (C) and copper (Cu) in the sample. However, it is noteworthy that the spectrum does exhibit unexpectedly prominent peaks of SiO_2 and oxygen (O), indicating the presence of significant surface contaminants. Upon the initiation of growth, the surface becomes entirely coated with silica, as evidenced by the SEM image. The binding energy versus intensity plot in Fig. 3 rules out the possibility of Cu_2O on the surface of the sample and demonstrates that the contamination is predominantly from SiO_2, and these findings are in agreement with the findings published by Ruiz et al.[32]

Improved, Contamination-Free Growth

To mitigate and prevent the introduction of quartz impurities during the growth process, modifications were made to the existing CVD setup. These modifications involved the incorporation of an alumina screen tube, as shown in Fig. 4, and the use of a sample holder made of alumina.

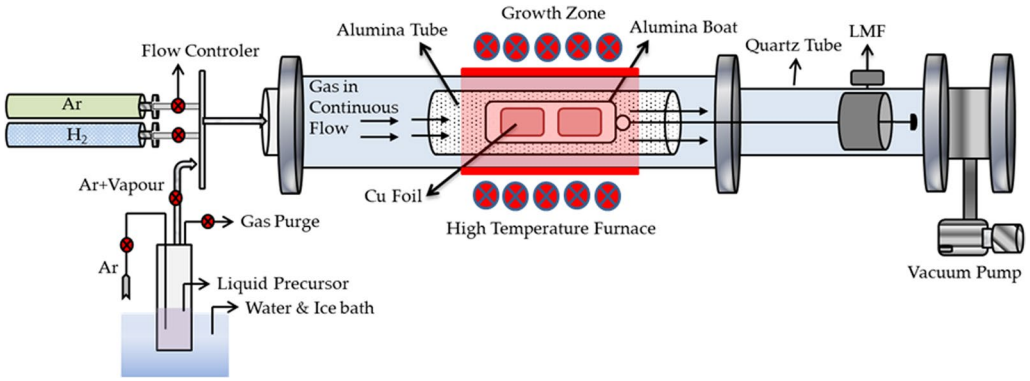

Fig. 4 Schematic of a redesigned CVD reactor.

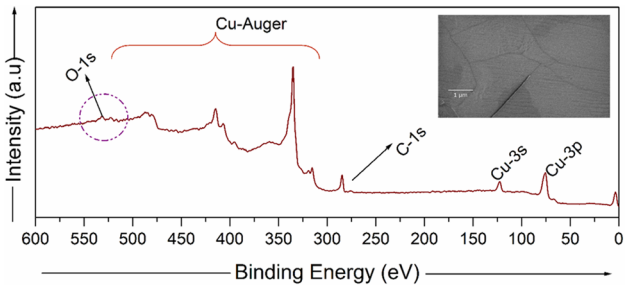

Fig. 5 XPS scan of graphene/Cu foil (the SEM image of freshly-deposited, uncontaminated graphene film is shown in the inset).

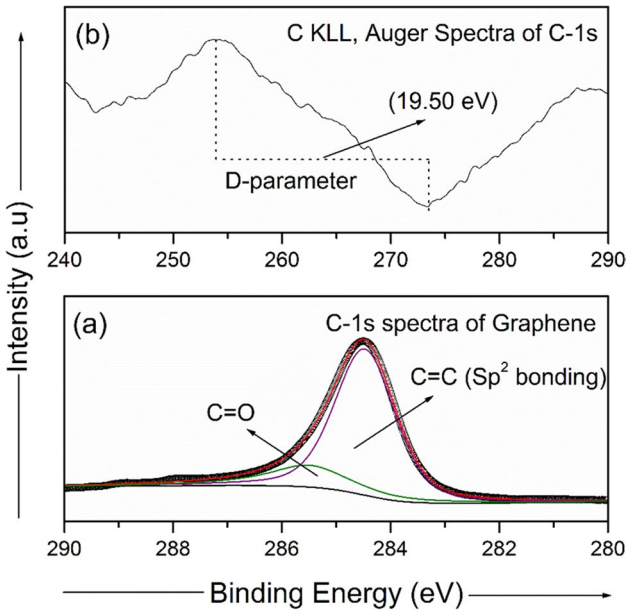

Fig. 6 (a) Core level and (b) C-KLL Auger spectra of graphene.

According to previous studies, alumina ceramic has a significantly higher melting temperature than quartz and exhibits superior thermochemical stability.[38,39] In contrast, alumina tubes exhibit higher thermal conductivity, facilitating improved heat transfer along the tube. However, this increased thermal conductivity renders them more vulnerable to thermal shocks, thereby increasing their susceptibility to failure in comparison to quartz tubes. The author resolved the issue by using a wider quartz vessel in conjunction with a smaller coaxial alumina tube that connects the two cooler ends of the reactor. This arrangement serves as a barrier to direct the SiO_x vapors toward the growth of the samples. Due to the rapid condensation of SiO_x vapors on the cooler surfaces of alumina tubes, their migration from the walls of the high-temperature quartz vessel to the hot samples is impeded. In addition, Cu atoms have little chance of penetrating alumina, and there should be no diffusional effects.[32] The gas precursors are managed by digitally controlled flow meters, while the pressure is adjusted by a needle valve on the opposite end of the tube. Ethanol is stored at 3 bars of pressure in an Ar-pressurized steel jar kept at 0°C (about 15 mbar of equilibrium pressure). It then enters the system by controlling the flow of argon gas. The alumina substrate holder is inserted and extracted from the high-temperature zone by use of a linear magnetic feedthrough (LMF) while the chamber is under vacuum.

After the growth, an XPS scan is performed to validate the cleanliness of the film. The resultant XPS survey spectrum of the graphene/Cu foil surface is displayed in Fig. 5. The spectrum shows no major peaks other than copper and carbon, indicating the deposited film is of high quality and free of contaminants. Figure 6a shows a core-level spectrum of C 1*s*, which allows us to identify the types of bonds that were present in the material. These spectrum characteristics may be assigned to distinct carbon-containing groups since they depend on the chemical environment of carbon atoms. The core level C 1*s* peak was de-convoluted, and it was found to be best fit by two peaks: one of these peaks belongs to graphitic C–C species centered at 284.5 eV, and the second small peak (C=O) at 285.5 eV.

It is always a difficult task to differentiate between sp^2/sp^3 hybridized carbons, since their binding energies are nearly overlapping. Therefore, the sp^2/sp^3 hybridization ratio is calculated differently. The carbon (C-KLL) Auger peak's width, which appears at a kinetic energy of 260 eV, is analyzed, and a metric known as the "D-parameter" is derived by finding the maxima and minima of the first derivative of the spectrum (as shown in Fig. 6b). According to the findings of Loscovich and colleagues, the D-parameter for sp^2 hybridized carbon is around 22 eV, whereas the D-parameter for sp^3 hybridized carbon is 13 eV.[40] In our particular instance, D-parameter and full width at half maximum (FWHM) values are 19.5 eV and 1.32 eV, respectively, and they follow the reported values of sp^2 hybridized carbon, demonstrating that the deposited layer on Cu is pure graphene.

Improved Transfer Process

The first and most crucial stage in the creation of CVD-grown graphene devices is the transfer of the as-prepared film from the growth substrate to the device-compatible target. It is, thus, critically important to maintain film quality throughout the transfer process, ensuring that the film remains free from contaminants, uniform, and unbroken. Graphene is typically protected with a temporary coating before being wet transferred onto a target substrate, etched, dried, and then the protective layer is removed as part of the normal wet chemical transfer process.[18] Various types of polymers, including poly(methyl methacrylate) (PMMA), polydimethylsiloxane (PDMS), and thermal release tapes, have been identified as supportive layers for the transfer of CVD graphene.[41,42] Among these options, the PMMA method has gained significant popularity and is commonly employed for this purpose. In the PMMA-based process, a layer of PMMA is applied through spin-coating onto a pre-existing graphene film, after which the metal component is subsequently removed via etching. Subsequently, the residual PMMA/graphene layer is transferred onto the designated substrate and subsequently eliminated using appropriate solvents. Additional processing steps have been implemented to enhance the efficiency of the transfer procedure.[43] The PMMA-assisted wet chemical transfer process, while being straightforward and efficient, presents significant concerns. Firstly, the utilization of solvents for PMMA removal poses a notable challenge. Secondly, the complete elimination of PMMA necessitates additional heat treatments, which can potentially compromise the quality of both the devices and the graphene film. Lastly, these processing steps are not compatible with a wide range of appropriate polymeric substrates. Therefore, to manufacture graphene-based products, it is imperative to develop a novel and sophisticated technique that is free of impurities, exhibits non-toxic characteristics, and effectively maintains the inherent properties of graphene.

In the given context, a notable prerequisite is to set up a transfer mechanism that is characterized by its simplicity, effectiveness, and ability to preserve the original characteristics of graphene sheets. Cyclododecane (CDD), a cyclic hydrocarbon, has the potential to serve as a viable substitute for various polymers such as PMMA and PDMS. The substance exhibits a high degree of hydrophobicity, displaying limited solubility in polar solvents such as water. It is characterized by its colorless and translucent appearance and is notable for its exceptional ability to form films. At standard ambient conditions, this organic compound, which is both non-toxic and environmentally friendly, exists in a solid state. Due to its specific characteristics, CDD exhibits complete sublimation upon exposure to air, rendering it a favored material for supporting and facilitating the transfer of graphene films.[44]

Figure 7 illustrates the graphene film synthesis and transfer mechanism, which is an eight-step process as discussed below:

Step 1- In the CVD process, the primary chemical reaction for graphene synthesis is the thermal decomposition of hydrocarbon (i.e., ethanol) in the presence of a carrier gas (H_2) at 1000°C. The carrier gas or reducing gas is used to ensure that no oxidation is taking place.
Step 2- This step involves the transport of carbon species to the substrate (adsorption), followed by surface migration and finally the formation of graphene film (nucleation and growth process).
Step 3- An oxygen plasma treatment is used to remove graphene from the back of the Cu substrate.
Step 4- Next, a thin layer of CDD diluted in ethyl ether is spin-coated onto the surface of graphene. By controlling the dilution and the number of drops, one may deposit homogeneous layers of CDD and achieve the optimal crystallite size.
Step 5- Subsequently, Cu is then etched with a 50 g/L solution of aqueous ammonium per-sulphate. The 25 µm-thick Cu foil is entirely etched away in less than 3 h at RT.
Step 6- The Graphene/CDD film is then thoroughly rinsed with DI water to get rid of any remaining residue from the manufacturing process.
Step 7- The Graphene/CDD stack is then transferred to a hydrophilic SiO_2 (300 nm)/Si target substrate that has been treated with oxygen plasma. The CDD/graphene/SiO_2 (300nm) is then heated to 70°C in the air to remove any remaining CDD and interfacial water trapped beneath the graphene. Since CDD melts at about 63°C, it should lower the surface tension at this last stage, making transfer easier and better.

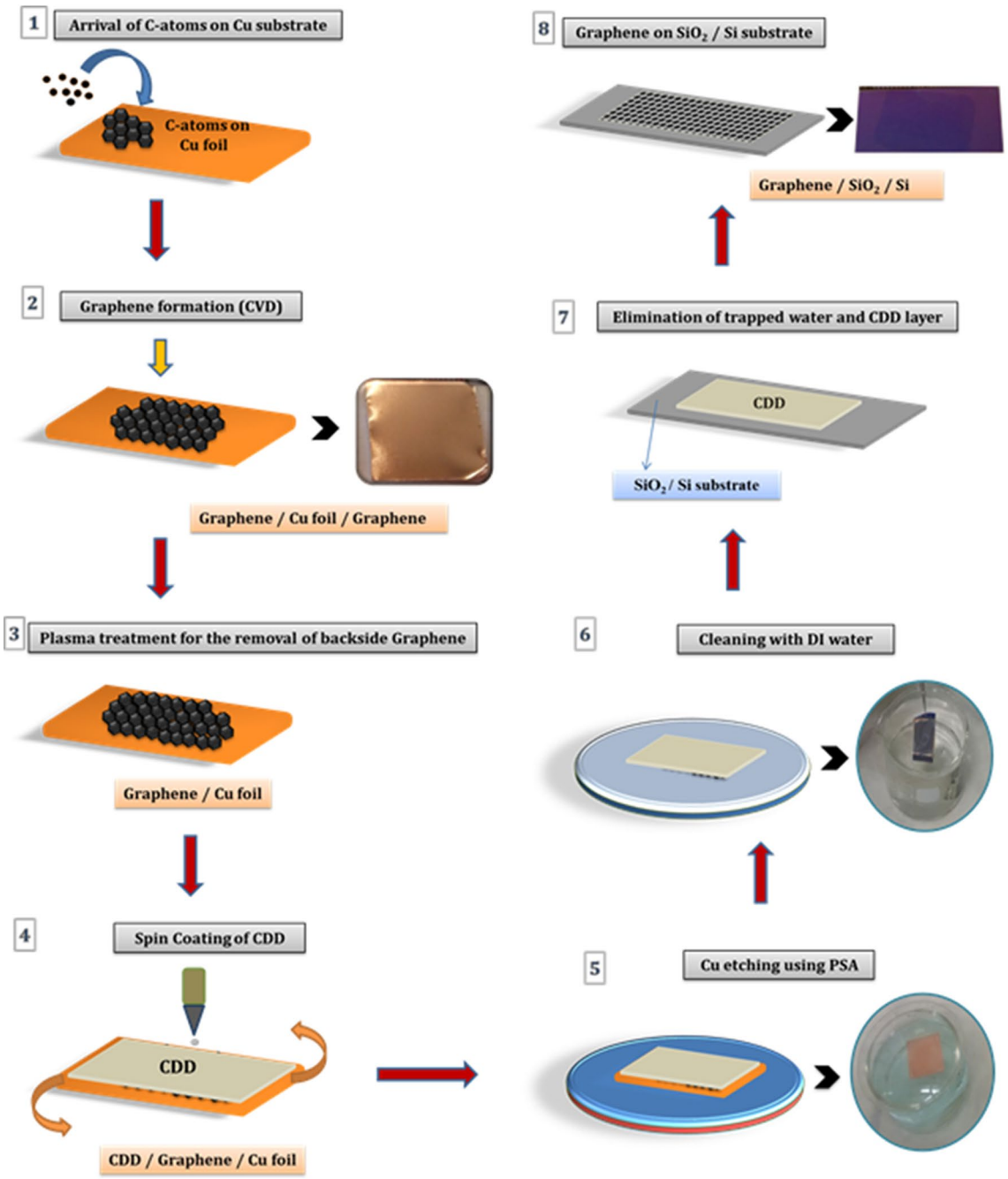

Fig. 7 Schematic of chemical vapor synthesis and transfer of monolayer graphene.

Step 8- Finally, high-quality graphene film is transferred to the SiO_2/Si substrate as shown in Fig. 7.

To ensure that the cleaning and transfer process did not compromise the quality of the graphene film, the samples were thoroughly characterized by Raman spectroscopy, which is one of the most effective, nondestructive, and widely used techniques for determining the structural properties, types of bonding, level of disorder, thickness, and number of stacked graphene sheets in layered graphene-like materials.[45,46] The spectral features of graphene exhibited three distinct peaks (D, G, and 2D), whose positions, widths, and heights can be used to quantify the various properties of the substance.[47]

Figure 8 illustrates the Raman spectra of CDD-transferred, contaminated, and clean graphene films after Cu etching using a 532 nm (2.33 eV) laser line. The spectrum of contaminated graphene film is dominated by two narrow

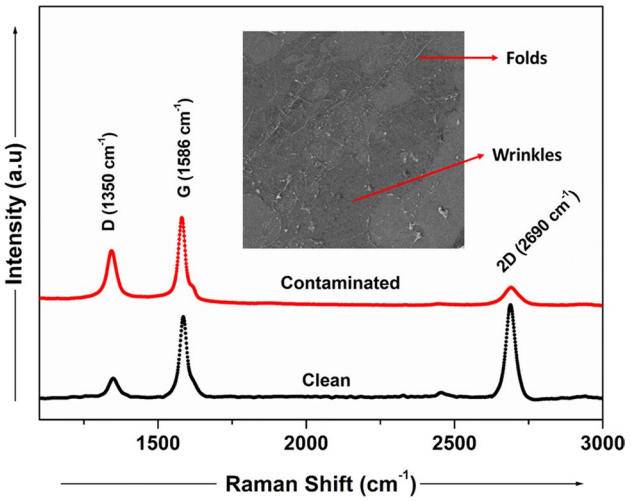

Fig. 8 Raman spectra of CDD-transferred contaminated and clean graphene films after Cu etching. Inset shows the SEM image of a clean graphene film transferred onto Si/SiO_2

peaks, D and G, centered at 1344 cm^{-1} and 1580 cm^{-1}, respectively. In addition to these peaks, the spectrum displays a broad, low-intensity peak at 2690.4 cm^{-1}, which corresponds to the 2D band. In contrast, the spectrum of clean graphene differs significantly from that of a contaminated graphene film. Here, the intensity of the 2D peak increases significantly to its maximum, while the intensity of the D peak decreases to its minimum. It is worth mentioning that the G and 2D band peaks of a clean graphene film are found to be quite close to those of a micromechanically exfoliated graphene film, indicating that the film synthesized by the modified assembly provides the desired result. This is an extremely important finding when dealing with graphene transferred using a supporting layer, as residues of the supporting material (such as PMMA) are always left behind after the transfer process, which significantly affects the graphene and device characteristics. Furthermore, the intensity ratio (I_{2D}/I_G) from the Raman spectrum may be used not only to assess the quality of graphene film but also to estimate the number of layers. A high (I_{2D}/I_G) ratio and a relatively small amplitude of the D peak indicate that graphene of high quality has been synthesized.[48] Table I shows the data obtained from the Raman spectrum for estimating the number of layers of graphene on a Si/SiO_2 substrate. The ratio of (I_{2D}/I_G) is 0.61 for contaminated graphene film and 1.15 for clean graphene film, as shown in Table I. Intensity ratio > 1 implies that the modified CVD system is successfully able to produce high-quality few layers of graphene film. Additionally, the intensity ratio (I_D/I_G) can be used for characterizing the defect quantity in graphene and also as an indicator of the film's crystalline quality. Here, the (I_D/I_G) ratio is found to be ~ 0.815 for contaminated and ~ 0.23 for clean graphene film, indicating that the sample produced via the modified

Table I Data obtained from Raman spectrum for estimating the number of layers of graphene on SiO_2/Si substrate

Graphene on SiO_2/Si	I_D/I_G	I_{2D}/I_G	La, nm
Contaminated	0.81	0.61	23.59
Clean	0.23	1.15	83.58

setup contains few defects. These defects may be the result of irregularities, edges, charged impurities, the presence of domain boundaries, or molecular folding.

The graphene domain size is estimated using the following equation:

$$L_a(\text{nm}) = (2.4 \times 10^{-10})\lambda_{\text{Laser}}^4 \left(\frac{I_D}{I_G}\right)^{-1},$$

where λ = laser is the wavelength of the excitation laser. The above formula is based on the Tuinstra–Koenig relation to calculate the crystallite size using Raman spectroscopy.[49] The large grain size of graphene ~ 83.58 nm suggests that the high-quality graphene film was successfully transferred onto a SiO_2/Si substrate by the wet chemical etching process, synthesized via a modified CVD system.

The inset of Fig. 8 also shows the SEM image of a corresponding transferred graphene film. There are fewer contaminants on the surface of the film, and it looks more continuous except for a few wrinkles and folds that form when the film cools down after synthesis because graphene and copper have different thermal expansion coefficients. These results further imply that this approach is capable of producing a much cleaner, continuous graphene film transfer with just a small amount of solvents being required during the spin coating process.

Conclusions

In summary, contamination-free graphene presents substantial potential across a spectrum of energy applications, spanning from storage and conversion to harvesting and catalysis. However, the commercial fabrication of high-grade graphene sheets for a range of applications has proven to be a significant barrier for makers, despite the undeniable promise of graphene's potential. In the present work, the authors presented a potential solution, which is demonstrated by the implementation of a quartz reactor and a vessel with an improved design. Moreover, the authors presented a rapid, annealing, and chemical etching-free method for transferring high-quality CVD graphene onto desirable surfaces. Raman, SEM, and XPS techniques were used to ensure the quality of the grown graphene film.

Acknowledgments The author (R.B.) would like to acknowledge ENEA for providing the International Research Fellowship. G.D. would like to acknowledge UPES for providing the PhD fellowship and research facilities.

Author contributions Gargi Dhiman: investigation, data curation, methodology, writing—original draft preparation. Shalendra Kumar and Ranjeet Brajpuriya: supervision, writing—review & editing.

Conflict of interest The authors declare that they have no known competing financial interests or personal relationships that could have appeared to influence the work reported in this paper.

References

1. S. Tkachev, M. Monteiro, J. Santos, E. Placidi, M. Hassine, P. Marques, P. Ferreira, P. Alpuim, and A. Capasso, Environmentally friendly graphene inks for touch screen sensors. *Adv. Funct. Mater.* 31, 2103287 (2021).
2. F. Withers, O. Del, A. Mishchenko, A. Rooney, A. Gholinia, K. Watanabe, T. Taniguchi, S. Haigh, A. Geim, A. Tartakovskii, and K. Novoselov, Light-emitting diodes by band-structure engineering in van der Waals heterostructures. *Nat. Mater.* 14, 301 (2015).
3. C. Lee, X. Wei, J. Kysar, and J. Hone, Measurement of the elastic properties and intrinsic strength of monolayer graphene. *Science* 321, 385 (2008).
4. S. Tiwari, S. Sahoo, N. Wang, and A. Huczko, Graphene research and their outputs: Status and prospect. *J. Sci.: Adv. Mater. Dev.* 5, 10 (2020).
5. G. Ak, Graphene: status and prospects. *Science* 324, 1530 (2009).
6. R. Capaz, Grand challenges in graphene and graphite research. 1 (2022).
7. G. Wang, L. Zhang, and J. Zhang, A review of graphene synthesis at low temperatures by CVD methods. *New Carbon Mater.* 35, 193 (2020).
8. Z. Hu, F. Li, H. Wu, J. Liao, Q. Wang, G. Chen, Z. Shi, Y. Zhu, S. Bu, Y. Zhao, M. Shang, Q. Lu, K. Jia, Q. Xie, G. Wang, X. Zhang, Y. Zhu, H. Wu, H. Peng, L. Lin, and Z. Liu, Rapid and scalable transfer of large-area graphene wafers. *Adv. Mater.* 35, 2300621 (2023).
9. H. Ci, J. Chen, H. Ma, X. Sun, X. Jiang, K. Liu, J. Shan, X. Lian, B. Jiang, R. Liu, B. Liu, G. Yang, W. Yin, W. Zhao, L. Huang, T. Gao, J. Sun, and Z. Liu, Transfer-free quasi-suspended graphene grown on a Si Wafer. *Adv. Mater.* 34, 2206389 (2022).
10. B. Liu, Z. Sun, K. Cui, Z. Xue, Z. Li, W. Wang, W. Gu, K. Zheng, R. Liu, Y. Zhao, M. Rummeli, X. Gao, J. Sun, and Z. Liu, Self-aided batch growth of 12-inch transfer-free graphene under free molecular flow. *Adv. Funct. Mater.* 33, 2210771 (2023).
11. B. Jiang, D. Liang, Z. Sun, H. Ci, B. Liu, Y. Gao, J. Shan, X. Yang, M. Rummelil, J. Wang, T. Wei, J. Sun, and Z. Liu, Toward direct growth of ultra-flat graphene. *Adv. Funct. Mater.* 32, 2200428 (2022).
12. J. Li, M. Chen, A. Samad, H. Dong, A. Ray, J. Zhang, X. Jiang, U. Schwingenschlogl, J. Domke, C. Chen, Y. Han, T. Fritz, R. Ruoff, B. Tian, and X. Zhang, Wafer-scale single-crystal monolayer graphene grown on sapphire substrate. *Nat. Mater.* 21, 740 (2022).
13. K. Novoselov, A. Geim, S. Morozov, D. Jiang, Y. Zhang, S. Dubonos, I. Grigorieva, and A. Firsov, Electric field in atomically thin carbon films. *Science* 306, 666 (2004).
14. H. Matte, K. Subrahmanyam, and C. Rao, Synthetic aspects and selected properties of graphene. *Nanomater. Nanotechnol.* 1, 5 (2011).
15. M. Bhuyan, M. Uddin, M. Islam, F. Bipasha, and S. Hossain, Synthesis of graphene. *Int. Nano Lett.* 6, 65 (2016).
16. L. Lin, H. Peng, and Z. Liu, Synthesis challenges for graphene industry. *Nat. Mater.* 18, 520 (2019).
17. J. Evans, P. Thiel, and M. Bartelt, Morphological evolution during epitaxial thin film growth: formation of 2D islands and 3D mounds. *Surf. Sci. Rep.Rep.* 61, 1 (2006).
18. X. Li, W. Cai, J. An, S. Kim, J. Nah, D. Yang, R. Piner, A. Velamakanni, I. Jung, E. Tutuc, S. Banerjee, L. Colombo, and R. Ruoff, Large-area synthesis of high-quality and uniform graphene films on copper foils. *Science* 324, 1312 (2009).
19. L. Sun and B. Hong, Chemical vapour deposition. *Nat. Rev. Methods Primers* 1, 5 (2021). https://doi.org/10.1038/s43586-020-00005-y.
20. L. Gao, W. Ren, H. Xu, L. Jin, Z. Wang, T. Ma, L. Ma, Z. Zhang, Q. Fu, L. Peng, X. Bao, and H. Cheng, Repeated growth and bubbling transfer of graphene with millimeter-size single-crystal grains using platinum. *Nat. Commun.* 3, 1 (2012).
21. L. Lin, B. Deng, J. Sun, H. Peng, and Z. Liu, Bridging the gap between reality and ideal in chemical vapor deposition growth of graphene. *Chem. Rev.* 118, 9281 (2018).
22. S. Karamat, S. Sonusen, Y. Celik, E.O. Uysalli, and A. Oral, Synthesis of few layer single crystal graphene grains on platinum by chemical vapour deposition. *Prog. Nat. Sci. Mater. Int.* 25(4), 291 (2015).
23. S. Bhaviripudi, X. Jia, M. Dresselhaus, and J. Kong, Role of kinetic factors in chemical vapor deposition synthesis of uniform large area graphene using copper catalyst. *Nano Lett.* 10, 4128 (2010).
24. B. Zhang, W. Lee, R. Piner, I. Kholmanov, Y. Wu, H. Li, H. Ji, and R. Ruoff, Low-temperature chemical vapor deposition growth of graphene from toluene on electropolished copper foils. *ACS Nano* 6, 2471 (2012).
25. P. Zhao, A. Kumamoto, S. Kim, X. Chen, B. Hou, S. Chiashi, E. Einarsson, Y. Ikuhara, and S. Maruyama, Self-limiting chemical vapor deposition growth of monolayer graphene from ethanol. *J. Phys. Chem. C* 117, 10755 (2013).
26. A. Gnisci, G. Faggio, G. Messina, J. Kwon, J. Lee, G. Lee, T. Dikonimos, N. Lisi, and A. Capasso, Ethanol-CVD Growth of sub-mm single-crystal graphene on flat Cu Surfaces. *J. Phys. Chem. C* 122, 28830 (2018).
27. Faggio G., Capasso A., Malara A., Leoni E., Nigro M. A., Santangelo S., Messina, T. Dikonimos, F. Buonocore, and N. Lisi. (2014). Fast growth of polycrystalline graphene by chemical vapor deposition of ethanol on copper. In: 2014 IEEE 9th Nanotechnology Materials and Devices Conference (NMDC) (pp. 69-72). IEEE.
28. S. Chaitoglou and E. Bertran, Control of the strain in chemical vapor deposition-grown graphene over copper via H_2 flow. *J. Phys. Chem. C* 120, 25572 (2016).
29. G. Faggio, G. Messina, C. Lofaro, N. Lisi, and A. Capasso, Recent advancements on the CVD of graphene on copper from ethanol vapor. *Journal of Carbon Research.* 6, 14 (2020).
30. P. Bøggild, Research on scalable graphene faces a reproducibility gap. *Nat. Commun.* 14, 1 (2023).
31. N. Lisi, T. Dikonimos, F. Buonocore, M. Pittori, R. Mazzaro, R. Rizzoli, S. Marras, and A. Capasso, Contamination-free graphene by chemical vapor deposition in quartz furnaces. *Sci. Rep.* 7, 1 (2017).
32. I. Ruiz, W. Wang, A. George, C. Ozkan, and M. Ozkan, Silicon oxide contamination of graphene sheets synthesized on copper substrates via chemical vapor deposition. *Adv. Sci. Eng. Med.* 6, 1 (2014).
33. G. Van Tendeloo, J. Van Landuyt, and S. Amelinckx, The α→β phase transition in quartz and $AlPO_4$ as studied by electron microscopy and diffraction. *Physica Status Solidi (a)* 33(2), 723 (1976).

34. A. Wright and M. Lehmann, The structure of quartz at 25 and 590°C determined by neutron diffraction. *J. Solid State Chem.* 36, 371 (1981).
35. B. Bunker, Molecular mechanisms for corrosion of silica and silicate glasses. *J. Non Cryst. Solids* 179, 300 (1994).
36. M. Asif, Y. Tan, L. Pan, J. Li, M. Rashad, and M. Usman, Thickness controlled water vapors assisted growth of multilayer graphene by ambient pressure chemical vapor deposition. *J. Phys. Chem. C* 119, 3079 (2015).
37. M. Losurdo, M. Giangregorio, P. Capezzuto, and G. Bruno, Graphene CVD growth on copper and nickel: role of hydrogen in kinetics and structure. *Phys. Chem. Chem. Phys.* 13, 20836 (2011).
38. F. Pawel, M. Rozmus, and B. Smuk, Properties of alumina ceramics obtained by conventional and non-conventional methods for sintering ceramics. *J. Achiev. Mater. Manuf. Eng.* 48, 29 (2011).
39. P.K. Panda, V.A. Jaleel, and G. Lefebvre, Thermal shock study of α-alumina doped with 0.2% MgO. *Mater. Sci. Eng. A* 485(1–2), 558 (2008).
40. L. Lascovich, R. Giorgi, and S. Scaglione, Evaluation of the sp2/sp3 ratio in amorphous carbon structure by XPS and XAES. *Appl. Surf. Sci.* 47, 17 (1991).
41. A. Pirkle, J. Chan, A. Venugopal, D. Hinojos, C.W. Magnuson, S. McDonnell, and R.M. Wallace, The effect of chemical residues on the physical and electrical properties of chemical vapor deposited graphene transferred to SiO_2. *Appl. Phys. Lett.* 99(12), 122108 (2011).
42. J. Park, W. Jung, D. Cho, J. Seo, Y. Moon, S. Woo, C. Lee, C. Park, and J. Ahn, Simple, green, and clean removal of a poly(methyl methacrylate) film on chemical vapor deposited graphene. *Appl. Phys. Lett.* 103, 171609 (2013).
43. X. Liang, B. Sperling, I. Calizo, G. Cheng, C. Hacker, Q. Zhang, Y. Obeng, K. Yan, H. Peng, Q. Li, X. Zhu, H. Yuan, A. Walker, Z. Liu, L. Peng, and C. Richter, Toward clean and crackless transfer of graphene. *ACS Nano* 5, 9144 (2011).
44. A. Capasso, M. Francesco, E. Leoni, T. Dikonimos, F. Buonocore, L. Lancellotti, E. Bobeico, M. Sarto, A. Tamburrano, G. Bellis, and N. Lisi, Cyclododecane as support material for clean and facile transfer of large-area few-layer graphene. *Appl. Phys. Lett.* 105(11), 113101 (2014).
45. A. Ferrari and J. Robertson, Raman spectroscopy of amorphous, nanostructured, diamondlike carbon, and nanodiamond. *Philos. Trans. Royal Soc. London Series: A Math. Phys. Eng. Sci.* 362, 2477 (2004).
46. G. Rimkute, M. Gudaitis, J. Barkauskas, A. Zarkov, G. Niaura, and J. Gaidukevic, Synthesis and characterization of graphite intercalation compounds with sulfuric acid. *Crystal* 12, 421 (2022).
47. A. Ferrari, J. Meyer, V. Scardaci, C. Casiraghi, M. Lazzeri, F. Mauri, S. Piscanec, D. Jiang, K. Novoseloc, S. Roth, and A. Geim, Raman spectrum of graphene and graphene layers. *Phys. Rev. Lett.* 97(18), 187401 (2006).
48. H. Zhou, W. Yu, L. Liu, R. Cheng, Y. Chen, X. Huang, Y. Liu, Y. Wang, Y. Huang, and X. Duan, Chemical vapour deposition growth of large single crystals of monolayer and bilayer graphene. *Nat. Commun.* 4, 2096 (2013).
49. F. Tuinstra and J.L. Koenig, Raman spectrum of graphite. *J. Chem. Phys.* 53(3), 1126 (1970).